J|A|C|S ARTICLES

Published on Web 05/05/2009

Role of Covalent Defects on Phonon Softening in Metallic Carbon Nanotubes

Khoi T. Nguyen and Moonsub Shim*

Department of Materials Science and Engineering, University of Illinois, Urbana, Illinois 61801

Received January 20, 2009; E-mail: mshim@illinois.edu

Abstract: We have examined how electrical characteristics and charging dependent Raman G-band phonon softening in individual metallic carbon nanotubes are influenced by covalent defects. In addition to decreasing electrical conductance with increasing on/off current ratio eventually leading to semiconducting behavior, adding covalent defects reduces the degree of softening and broadening of longitudinal optical (LO) phonon mode of the G-band near the charge neutrality point where the bands cross. On the other hand, the transverse optical (TO) mode softening is enhanced by defects. Implications on the interpretation of Raman G-band phonon softening and on utilizing Raman spectroscopy to examine covalent functionalization are discussed.

Introduction

Raman spectroscopy continues to be a key characterization technique for elucidating physics and chemistry of carbon materials, especially carbon nanotubes and graphene.[1,2] Hence, understanding Raman active phonon modes and how they are affected by processes such as charging,[3] electron−phonon coupling,[4,5] and chemical functionalization[6] are in turn important in defining and assessing these unique materials' applicability in new and developing technologies. One recent focus has been on the effect of electron−phonon coupling on the G-band phonon frequencies and lineshapes/linewidths. Both graphene and metallic single-walled carbon nanotubes (SWNTs) exhibit G-band phonon softening and broadening when the Fermi level lies near the charge neutrality point, the Dirac point.[5,7−10] Due to their one-dimensional nature, this phonon softening effect is more enhanced in metallic SWNTs. For metallic SWNTs, it is the G-band LO mode that becomes softened due to this coupling of phonons to conduction electron excitations. The TO mode is not expected to exhibit such electron−phonon coupling effects which leads to the LO mode frequency being lower than that of the TO mode.[7] This assignment of the two main features of the G-band of metallic SWNTs is now generally accepted and, to a large extent, how the LO mode frequency and line width evolve with charging has been explained by this strong electron−phonon coupling effect.[7] However, complications remain in interpreting experimental results. For example, a wide distribution of phonon frequencies and linewidths even within a single chirality makes it difficult to determine the intrinsic phonon linewidths and frequencies that can be compared to theoretical predictions.[11] While much of the distribution has been shown to arise from the variations in the Fermi level position (charging) with one key cause being exposure to ambient oxygen, there is no obvious relation between the degree of charging and the degree of disorder, both of which appear upon oxygen exposure.[8,11,12] Another complication is in whether or

(1) Dresselhaus, M. S.; Dresselhaus, G.; Hofmann, M. *Vib. Spectrosc.* **2007**, *45*, 71.
(2) Ferrari, A. C. *Sol. State Comm.* **2007**, *143*, 47.
(3) (a) Rao, A. M.; Eklund, P. C.; Bandow, S.; Thess, A.; Smalley, R. E. *Nature* **1997**, *388*, 257. (b) Kazaoui, S.; Minami, N.; Matsuda, N.; Kataura, H.; Achiba, Y. *Appl. Phys. Lett.* **2001**, *78*, 3433. (c) Kavan, L.; Rapta, P.; Dunsch, L.; Bronikowski, M. J.; Willis, P.; Smalley, R. E. *J. Phys. Chem. B* **2001**, *105*, 10764. (d) Kavan, L.; Dunsch, L. *Nano Lett.* **2003**, *3*, 969.
(4) (a) Charlier, J.-C.; Eklund, P. C.; Zhu, J.; Ferrari, A. C. *Topics Appl. Phys.* **2008**, *111*, 673. (b) Maultzsch, J.; Reich, S.; Thomsen, C. *Phys. Rev. B* **2002**, *65*, 233402. (c) Souza Filho, A. G.; Jorio, A.; Samsonidze, G. G.; Dresselhaus, G.; Saito, R.; Dresselhaus, M. S. *Nanotech.* **2003**, *14*, 1130. (d) Oron-Carl, M.; Hennrich, F.; Kappes, M. M.; Lohneysen, H. V.; Krupke, R. *Nano Lett.* **2005**, *5*, 1761. (e) Hartman, A. Z.; Jouzi, M.; Barnett, R. L.; Xu, J. M. *Phys. Rev. Lett.* **2004**, *92*, 236804. (f) Tsang, J. C.; Freitag, M.; Perebeinos, V.; Liu, J.; Avouris, Ph. *Nat. Nanotech.* **2007**, *2*, 725.
(5) (a) Yan, J.; Zhang, Y.; Kim, P.; Pincruk, A. *Phys. Rev. Lett.* **2007**, *98*, 166802. (b) Pisana, S.; Lazzeri, M.; Casiraghi, C.; Novoselov, K. S.; Geim, A. K.; Ferrari, A. C.; Mauri, F. *Nat. Mater.* **2007**, *6*, 198. (c) Abdula, D.; Ozel, T.; Kang, K.; Cahill, D. G.; Shim, M. *J. Phys. Chem. C* **2008**, *112*, 20131.
(6) (a) Wang, C.; Cao, Q.; Ozel, T.; Gaur, A.; Rogers, J. A.; Shim, M. *J. Am. Chem. Soc.* **2005**, *127*, 11460. (b) Kamaras, K.; Itkis, M. E.; Hu, H.; Zhao, B.; Haddon, R. C. *Science* **2003**, *301*, 1501. (c) Chattopadhyay, D.; Galeska, I.; Papadimitrakopoulos, F. *J. Am. Chem. Soc.* **2003**, *125*, 3370. (d) Strano, M. S.; Dyke, C. A.; Usrey, M. L.; Barone, P. W.; Allen, M. J.; Shan, H.; Kittrell, C.; Hauge, R. H.; Tour, J. M.; Smalley, R. E. *Science* **2003**, *301*, 1519. (e) An, K. H.; Park, J. S.; Yang, C.-M.; Jeong, S. Y.; Lim, S. C.; Kang, C.; Son, J.-H.; Jeong, M. S.; Lee, Y. H. *J. Am. Chem. Soc.* **2005**, *127*, 5196. (f) Kanungo, M.; Lu, H.; Malliaras, G.; Blanchet, G. B. *Science* **2009**, *323*, 234.
(7) (a) Piscanec, S.; Lazzeri, M.; Mauri, M.; Ferrari, A. C.; Robertson, J. *Phys. Rev. Lett.* **2004**, *93*, 185503. (b) Lazzeri, M.; Piscanec, S.; Mauri, F.; Ferrari, A. C.; Robertson, J. *Phys. Rev. B* **2006**, *73*, 155426. (c) Piscanec, S.; Lazzeri, M.; Robertson, J.; Ferrari, A. C.; Mauri, F. *Phys. Rev. B* **2007**, *75*, 035427. (d) Caudal, N.; Saitta, A. M.; Lazzeri, M.; Mauri, F. *Phys. Rev. B* **2007**, *75*, 115423. (e) Das, A.; Sood, A. K.; Govindaraj, A.; Saitta, A. M.; Lazzeri, M.; Mauri, F.; Rao, C. N. R. *Phys. Rev. Lett.* **2007**, *99*, 136803.
(8) Nguyen, K. T.; Gaur, A.; Shim, M. *Phys. Rev. Lett.* **2007**, *98*, 145504.
(9) Wu, Y.; Maultzsch, J.; Knoesel, E.; Huang, M.; Sfeir, M. Y.; Brus, L. E.; Hone, J.; Heinz, T. F. *Phys. Rev. Lett.* **2007**, *99*, 027402.
(10) Frahat, H.; Son, H.; Samsonidze, G. G.; Reich, S.; Dresselhaus, M. S.; Kong, J. *Phys. Rev. Lett.* **2007**, *99*, 145506.
(11) Shim, M.; Gaur, A.; Nguyen, K. T.; Daner, A.; Ozel, T. *J. Phys. Chem. C* **2008**, *112*, 13017.
(12) Gaur, A.; Shim, M. *Phys. Rev. B* **2008**, *78*, 125422.

not the TO mode softens. There have been apparent discrepancies in experimentally observed behavior of the TO mode—that is, some reports show TO mode softening,[8,10] some show that it does not,[7] yet others show both behaviors.[13] While progress is being made in understanding charging dependent Raman spectral changes, very little attention has been given on how disorder complicates these spectral changes. Beyond the increasing D-band intensity and the appearance of the so-called D' shoulder at the high frequency side of the G-band, only limited information about how covalent reactions alter Raman spectra is available. Given that significant percentage of, if not most, individual metallic SWNTs exhibit measurable D-band intensities,[11,14] establishing the role of existing physical disorder on the observe Raman spectral response upon charging is necessary. Such information is also critical especially in characterizing chemical functionalization and doping processes that involve charge transfer.

Simultaneous Raman and electrochemical gating studies on single isolated metallic SWNTs at different stages of covalent defect introduction (i.e., following the same SWNT while increasing degree of disorder) may separate out the role of disorder from charging effects on the Raman active modes of SWNTs. Here, we introduce increasing degree of covalent defects via reaction with increasing concentration of 4-bromobenzene diazonium tetrafluoroborate (4-BBDT) and examine the charging dependent G-band Raman spectral evolution of individual metallic SWNTs after each reaction step with 4-BBDT. This choice of the chemical reagent for introducing defects may also lead to further insights in developing simple scalable electronically selective chemistry for SWNTs since 4-BBDT has shown some selectivity toward metallic SWNTs.[6a,d,15,16] Adding covalent chemical groups to the sidewalls influences not only the electronic properties but also the phonon characteristics.[17] Therefore, chemical functionalization may facilitate pathways to electronic and phonon band structure engineering in addition to selectively sorting out metallic and semiconducting SWNTs for nanoelectronics and sensor applications. Reaction with 4-BBDT is presumably initiated by charge transfer[6d] and may shift the Fermi level of SWNTs. Such Fermi level shifts, as we show here, can complicate comparisons between Raman features before and after the reaction because the Raman modes are both charge and defect dependent. By measuring Raman spectra at different electrostatic doping levels, we can directly examine how Raman spectra at the same Fermi level position, especially near the charge neutrality point, evolve with increasing covalent defects. Changes in charging dependent softening of *both* LO and TO modes of metallic SWNTs are shown. Softening of the TO mode is enhanced by the introduced defects. Implications on comparing expected and experimentally observed G-band phonon softening and on Raman characterization of covalent functionalization are discussed.

Experimental Section

Synthesis and fabrication processes have been described elsewhere.[8] Briefly, SWNTs were grown by chemical vapor deposition with patterned catalysts on heavily doped Si substrates with 300 nm thermal oxide. Gold electrodes with Ti wetting layer were deposited on top of the SWNTs. In addition to allowing electrical measurements, these electrodes also serve as markers to ensure that the same nanotube is measured via Raman spectroscopy. Electrochemical gate potential was applied with a nearby electrode through a 20 wt % $LiClO_4 \cdot 3H_2O$ in polyethylenimine (Aldrich, low molecular weight) spin coated on top of SWNT devices. This polymer electrolyte gate medium was removed by rinsing thoroughly with methanol before functionalizing SWNTs with 4-BBDT of indicated concentrations in distilled water for 15 min and then applied again for subsequent studies. Raman measurements were carried out on a JY LabRam HR 800 using a 1.96 eV excitation source through a 100x air objective (laser spot size $\sim$1 μm). Laser power was kept at or below $\sim$1 mW. For measurements under gate field, the samples were allowed to equilibrate at the applied gate voltage for $\sim$2 min prior to initiating Raman measurements. All measurements being on individual SWNTs are supported by consistent diameter measured by atomic force microscopy and radial breathing mode (RBM) in the Raman spectrum, only a single RBM peak being observed throughout the functionalization process, and by postmeasurement electrical breakdown showing a single cutting behavior (Supporting Information).

Results and Discussion

Figure 1a shows how the electrical conductance (normalized to the maximum conductance for comparison) of a metallic SWNT changes upon reaction with 4-BBDT. Unlike previous report using back gate configuration,[6a,15] polymer electrolyte gating allows nearly ideal gate efficiencies and the enhancement of gate dependence can actually be observed here (i.e., increasing maximum-current/minimum-current (on/off current) ratio from $\sim$2 before reaction to $\sim$300 after reacting with 50 μM 4-BBDT resulting in semiconductor-like behavior). However, there is a large overall decrease in the conductance from 1.6 μS to 1.4×10^{-2} μS as seen in Figure 1b. Figure 1b also shows that the integrated D/G intensity ratio (I_D/I_G) increases with increasing reaction concentration of 4-BBDT confirming introduction of covalent defects. Note that I_D/I_G includes the asymmetric Fano line shape of the G-band as described in ref 16.

In Figure 1c, we show the D- and the G-band regions of the Raman spectra of the metallic SWNT at each step of the reaction with 4-BBDT. The inset is the radial breathing mode (RBM) seen at 167 cm^{-1} before the reaction. Each spectrum is fitted with one Lorentzian for the D-band around 1320 cm^{-1} and one Fano line and three Lorentzians for the G-band. Following refs 8 and 12, we refer to the Fano peak labeled P1 as the LO mode and Loretzian peak labeled P3 as the TO mode. These spectra have been collected without any polymer electrolyte gate medium or external gate potential. Such a set of spectra may represent what would be usually measured following a chemical reaction of SWNTs—that is, without ensuring the same Fermi level position. With this particular metallic SWNT, we observe a significant increase in the G-band line width (LO line width Γ_{LO} increases from 28 to 53 cm^{-1}) along with a frequency downshift (LO frequency ω_{LO} shifts from 1556 to 1550 cm^{-1}) after the first reaction with 10 μM 4-BBDT. Here, all linewidths refer to full-width-at-half-maximum throughout. As Figure 1d indicates, these apparent changes turn out to be opposite of what

(13) Sasaki, K.; Saito, R.; Dresselhaus, G.; Dresselhaus, M. S.; Farhat, H.; Kong, J. *Phys. Rev. B* **2008**, *77*, 245441.
(14) Gao, B.; Zhang, Y.; Kong, J.; Liu, Z. *J. Phys. Chem. C* **2008**, *112*, 8319.
(15) (a) Balasubramanian, K.; Sordan, R.; Burghard, M.; Kern, K. *Nano Lett.* **2004**, *4*, 827. (b) An, L.; Fu, Q.; Lu, C.; Liu, J. *J. Am. Chem. Soc.* **2004**, *126*, 10520.
(16) Abdula, D.; Nguyen, K. T.; Shim, M. *J. Phys. Chem. C* **2007**, *111*, 17755.
(17) Fantini, C.; Pimenta, M. A.; Strano, M. S. *J. Phys. Chem. C* **2008**, *112*, 13150.

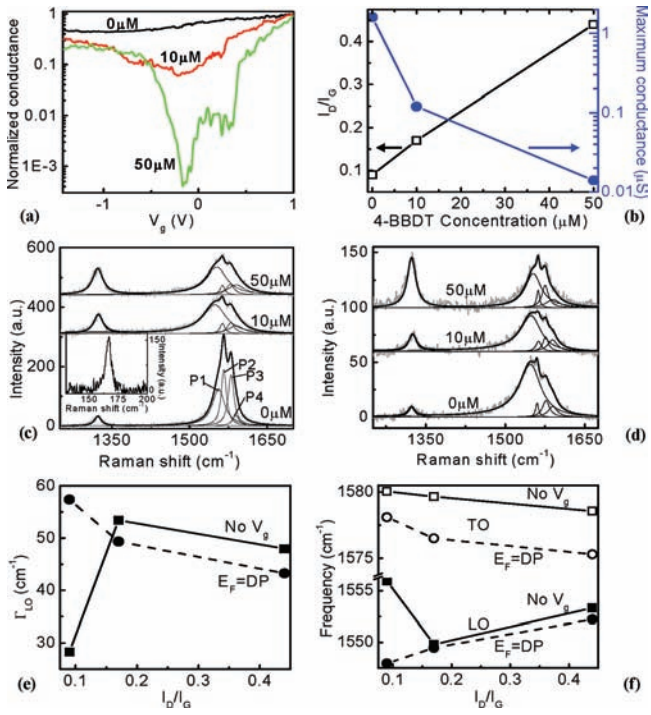

Figure 1. (a) Gate voltage (V_g) dependent electrical conductance of one metallic SWNT after reaction with indicated concentration of 4-BBDT. The conductance is normalized to the maximum conductance for comparison. "0 μM" refers to spectrum as fabricated before the reaction. (b) Integrated D/G intensity ratio (I_D/I_G) and maximum conductance vs reaction concentration of 4-BBDT. (c) Raman D- and G-band modes along with corresponding curve fits at different stages of covalent defect introduction without polymer electrolyte and without applied V_g. Curve fitting as described in the text is shown along with the spectra. Inset is the radial breathing mode region before reaction. (d) Raman spectra under polymer electrolyte gate potential where there is a conductance minimum with the maximum G-band line width (i.e., when all three cases have the Fermi level, E_F, at the Dirac point, DP). (e) Comparisons of LO mode line width change, Γ_{LO}, with (●) and without (■) fixing the E_F at DP. (f) Comparisons of changes in the LO and TO mode frequencies with (● = LO and ○ = TO) and without (■ = LO and □ = TO) fixing the E_F at DP.

actually happens when the Raman spectra are collected with applied electrochemical gate potential to ensure that the Fermi level lies near the Dirac point where the SWNT is charge neutral. Figures 1e and 1f indicate that, when spectra measured with Fermi level at the same position are compared, distinct trends of decreasing Γ_{LO} and increasing ω_{LO} with increasing degree of covalent reaction with 4-BBDT can be observed. Spectra collected at different gate voltages along with corresponding curve fits of this SWNT as-fabricated and after reaction with 50 μM 4-BBDT are shown in the Supporting Information. Figure 1f reveals that, unlike ω_{LO}, the TO mode frequency (ω_{TO}) exhibits a decreasing trend with increasing degree of covalent reaction with 4-BBDT. This observation is discussed further later. One important point already apparent from these results is that in order to characterize covalent reactions of SWNTs with Raman spectroscopy, one should ensure the same Fermi level position before and after the reaction. One should especially be careful not to hastily conclude loss of the G-band Fano component in an ensemble of SWNTs as loss of metallic tubes.

The gate voltage dependence of ω_{LO} and Γ_{LO} before any reaction and after reaction with 10 and 50 μM 4-BBDT are shown in Figure 2a and b. The qualitative dependence to charging is the same in all three cases. That is, the expected

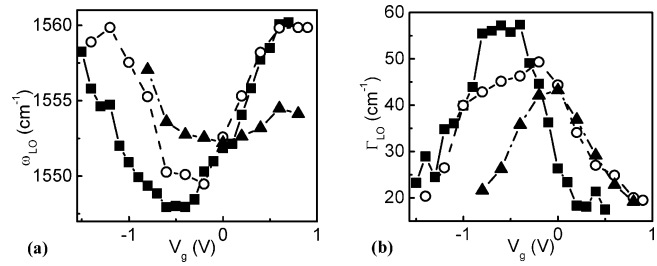

Figure 2. Gate dependence of G-band LO frequency (a) and line width (b) of the same metallic SWNT shown in Figure 1 after reaction with 0 (squares), 10 (circles), and 50 μM (triangles) 4-BBDT concentrations.

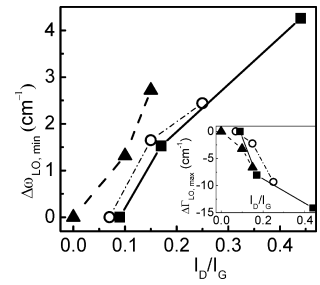

Figure 3. Integrated D/G intensity ratio dependence of change in LO mode frequency near the Dirac point for the SWNT shown in Figure 1 (squares), for another SWNT with similar RBM frequency (circles), and for a larger diameter SWNT with RBM at 105 cm^{-1} (triangles). Inset is the integrated D/G intensity ratio dependence of LO mode line width.

phonon softening and broadening of the LO mode occurs near the Dirac point at all stages of the covalent reaction. The difference lies in the degree of softening and broadening. The decreasing degree of phonon softening and broadening is shown for three different metallic SWNTs in Figure 3. The main panel is the change in the minimum ω_{LO} ($\Delta\omega_{LO,\ min}$). The inset is the change in the maximum Γ_{LO} ($\Delta\Gamma_{LO,\ max}$). Covalent functionalization can remove electronic states near the Dirac point and eventually open a band gap in metallic nanotubes.[18] Increasing defect density from covalent reaction with 4-BBDT then is likely to be reducing the density of states (DOS) near the Dirac point which in turn reduces free carrier density. The increasing gate dependence of conductance leading to semiconductor-like behavior after reaction with 50 μM 4-BBDT shown in Figure 1a supports the idea of reduction in DOS near the Dirac point. Carrier scattering from defects would decrease the overall conductivity but does not necessarily lead to enhanced gate dependence. The change in the electronic structure especially about the Dirac point then reduces the degree of electron−phonon coupling induced effects (i.e., alleviating the Kohn anomaly induced phonon softening and line broadening) leading to the observations in Figure 3 where the degree of LO phonon softening and broadening decreases with increasing covalent defect density.

While the LO mode exhibits behavior consistent with the gradual removal of Kohn anomaly induced phonon softening, increasing defect density leads to *enhanced* softening of the TO mode. Figure 4a shows how the gate dependence of ω_{TO} changes with covalent functionalization for the same metallic SWNT shown in Figure 1. Data for another metallic SWNT, which exhibits a larger change, is presented in Figure 4b. The G-band of this SWNT can be described fairly well with 2 peaks and

(18) Lee, Y.-S.; Nardelli, M. B.; Marzari, N. *Phys. Rev. Lett.* **2005**, *95*, 076804.

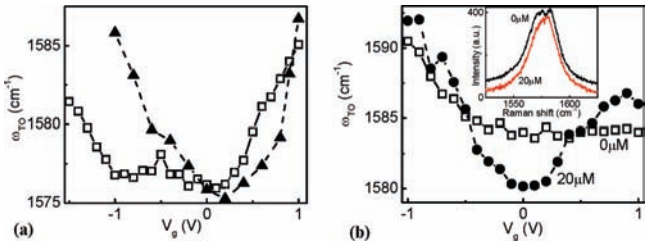

Figure 4. Gate dependence of TO frequency after reaction with 0 (squares) and 50 μM (triangles) 4-BBDT concentrations. Data for the same metallic SWNT as in figures 1 and 2 is shown (a) and another metallic SWNT with RBM at 105 cm^{-1} is shown in (b). Concentration of 4-BBDT is indicated for this SWNT. G-band spectra at $V_g = 0$ V (Fermi level near the Dirac point) is shown in the inset. The spectra are offset for clarity.

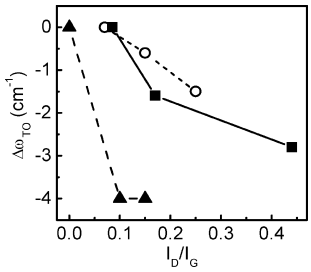

Figure 5. Integrated D/G intensity ratio dependence of change in TO mode frequency near the Dirac point for three SWNTs shown in Figure 3.

the fitting results are shown in the Supporting Information. The SWNT in Figure 4b initially exhibited no observable D-band intensity and the low degree of initial disorder in this SWNT may be the main reason for the larger change. Nevertheless, as Figure 5 indicates, all three metallic SWNTs examined here show the same trend of TO mode softening near the Dirac point with increasing defect density. Covalent functionalization introduces local sp^3 defects disrupting the sp^2 system and increasing the average bond length, which should then, in principle, lead to softening of all in-plane modes (i.e., both TO and LO modes). This defect induced softening is observed in TO mode which is expected to be independent of Kohn anomaly effects near the Dirac point. LO mode, on the other hand, exhibits stiffening with increasing defect density because the reduction in electron−phonon coupling induced effects is dominating the spectral changes.

In addition to the softening near the Dirac point, another notable change to TO mode upon covalent functionalization is that it stiffens much more readily upon charging. That is, a much larger change in ω_{TO} can be seen with smaller applied gate voltage when the SWNT is more defective. Because of the electron−phonon coupling matrix element for the TO mode being zero, initial theoretical studies have led to the expectation that TO mode does not soften like the LO mode and therefore ω_{TO} should be independent of charging.[7] However, both charge dependent and independent ω_{TO} have been observed experimentally.[8,10,13] Most recently, these apparently contradicting results have been suggested to arise from chirality-dependent behavior.[13] Achiral metallic SWNTs are expected to exhibit only LO mode softening. Chiral metallic SWNTs may exhibit softening of both LO and TO modes because the TO mode is not exactly along the circumferential direction.[13] This then leads to both ω_{LO} and ω_{TO} being dependent on the Fermi level position due to the Kohn anomaly. While such chirality dependent behavior can be expected, our results in Figures 4 and 5 indicate that the degree of disorder may sometimes have a larger influence on the observed softening of the TO mode.

Conclusions

We have shown that softening of both LO and TO modes of metallic SWNTs is sensitive not only to Fermi level position but also to the degree of disorder. With increasing defect density, LO mode stiffens whereas the TO mode softens. Softening of both LO and TO modes may be expected due to covalent defects changing hybridization of C atoms from sp^2 to sp^3 resulting in longer average bond lengths. However, LO mode exhibits stiffening rather than softening because it is already softened via coupling of the phonon with conduction electron excitations and the removal of this effect is the dominant change. These observations imply that reported experimental LO mode frequencies may be higher than the intrinsic frequencies due to the presence of physical disorder, which is observed via measurable D-band intensities in majority of individual metallic SWNTs. The degree of TO mode softening is also dependent on disorder and therefore sorting out possible chirality dependence should ensure that the defect induced changes have been separated out. Furthermore, monitoring chemical reactions that form covalent bonds via Raman spectroscopy should take into account both the Fermi energy position and disorder dependent changes in the Raman features. We suggest similar care to be taken into consideration for graphene.

Acknowledgment. This material is based upon work supported by NSF (Grants No. DMR-0348585 and No. CCF-0506660). K.T.N. acknowledges support from Vietnam Education Foundation.

Supporting Information Available: Raman spectra collected at different gate voltages along with corresponding curve fits for the SWNT shown in Figure 1 as-fabricated and after reaction with 50 μM 4-BBDT, electrical breakdown characteristics, and Raman spectra and curve fitting results of SWNT shown in Figure 4b. This material is available free of charge via the Internet at http://pubs.acs.org.

JA900461M